Final Report to NOAA/CPO/MAPP on the Project

Understanding atmosphere-ocean coupled processes in the southeast Pacific

Jialin Lin
The Ohio State University
(Award number: NA10OAR4310258)

1. Summary of activities

Our main activities are:

1. Process different long-term cloud datasets for studying stratocumulus clouds and feedback including ISCCP, MODIS, PATMOSX, SSMI, and ICOADS. Process large-scale environment datasets including CFSR reanalysis, ERA-Interim reanalysis, GPCP precipitation, ERSST and CERES radiative fluxes.
2. Process the CMIP5/CFMIP model simulations for all 8 models with complete ISCCP-simulator output. We use 27 years (model year 1979-2005) of the historical simulations of SST, large-scale atmosphere environment (temperature, humidity, and vertical motion), all sky and clear sky radiative fluxes, and cloud properties from ISCCP-simulator including total cloud cover, cloud top pressure (Ptop), cloud albedo, and Ptop-cloud optical depth (τ) histogram of cloud cover.
3. Evaluate the simulation of stratocumulus clouds in southeast Pacific by the CMIP5/CFMIP models.
4. Examine the cloud-radiation feedback associated stratocumulus clouds in southeast Pacific simulated by the CMIP5/CFMIP models.
5. Examine the causes of model biases in stratocumulus clouds and cloud-radiation feedback.
6. Explore the possible ways to improve the simulation of stratocumulus clouds and cloud-radiation feedback.

2. Major findings

1. The state-of-the-art global climate models still have significant difficulty in simulating the SEP stratocumulus clouds and associated cloud feedback. Comparing with observation, the models tend to simulate significantly less cloud cover, higher cloud top, and a variety of unrealistic cloud albedo.
2. The insufficient cloud cover leads to overly weak shortwave cloud radiative forcing (CRF) and net CRF.
3. Only two of the eight models capture the observed positive cloud feedback at sub-annual to decadal time-scales.
4. The cloud and radiation biases in the models are associated with (1) model biases in large-scale temperature structure including the lack of temperature inversion, insufficient lower troposphere stability (LTS), and insufficient reduction of LTS

with local SST warming, and (2) improper model physics especially insufficient increase of low cloud cover associated with larger LTS.

5. *Our results suggest that using cloud-top radiative cooling to drive boundary layer turbulence helps to improve the simulation of stratocumulus clouds and associated cloud feedback.*

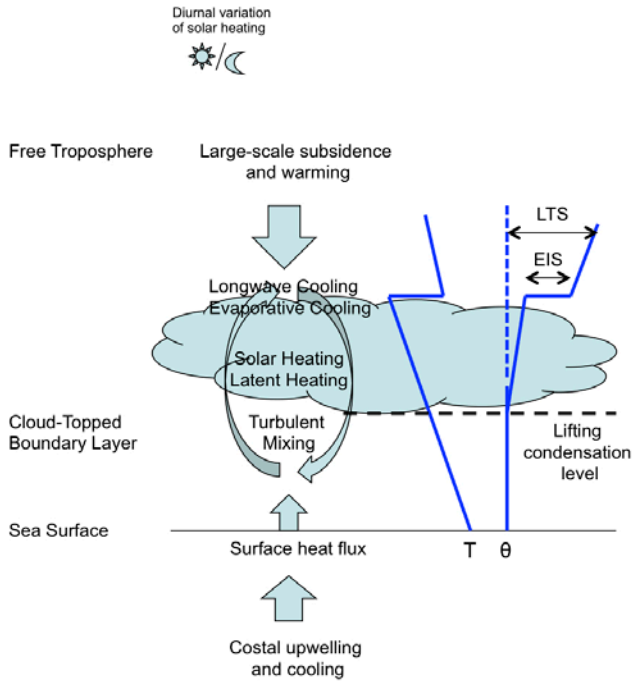

Figure 1. Schematic depiction of the lage-scale forcing and physical processes for stratocumulus-topped boundary layer. LTS is lower troposphere stability, and EIS is estimated inversion strength. From Lin et al. (2013).

3. Selected results

(1) Annual mean and seasonal cycle

Figure 2 shows the horizontal map of annual mean low cloud cover for (a) ISCCP observation and (b)-(i) eight CMIP5/CFMIP models. The observed clouds show a clear local maximum along the coast between 10ºS-30ºS and 270ºW-290ºW. Only two models (HAES and CAM5) produce a similar pattern but with much smaller cloud cover. All the other models simulate an overly small cloud cover and some of the models show a noisy spatial distribution (CANE, MIR5, and MPIE).

Figure 3 displays the vertical structure of clouds represented by the Ptop-τ histogram of annual mean cloud cover averaged between 10ºS-30ºS, 70ºW-90ºW. The observed clouds are dominated by low and middle clouds with cloud-top pressure higher than 560 mb, especially the stratocumulus clouds with cloud-top pressure between 680 mb and 800 mb

and τ between 3.6-23. Six of the eight models (CANE, HAES, MIR5, MPIE, MRIC, and CAM5) successfully reproduce the dominance of low and middle clouds, but the cloud covers tend to be smaller than observation. In the two IPSL models, however, the clouds are dominated by high clouds, especially cirrus and cirrostratus clouds.

Figure 4 displays the seasonal cycle of (a) SST, (b) total cloud cover, (c) cloud top pressure, (d) LTCC, (e) cloud albedo, (f) longwave CRF (LWCRF), (g) shortwave CRF (SWCRF), and (h) net CRF (NETCRF) averaged between 10ºS-30ºS, 70ºW-90ºW. Comparing with observation, the models tend to simulate significantly less cloud cover, higher cloud top, and a variety of unrealistic cloud albedo. The insufficient cloud cover leads to overly weak shortwave CRF and net CRF. All models simulate well the phase of the SST seasonal cycle, but only two models (HAES and CAM5) could capture the phases of seasonal cycle for LTCC, cloud albedo, SWCRF, and NETCRF.

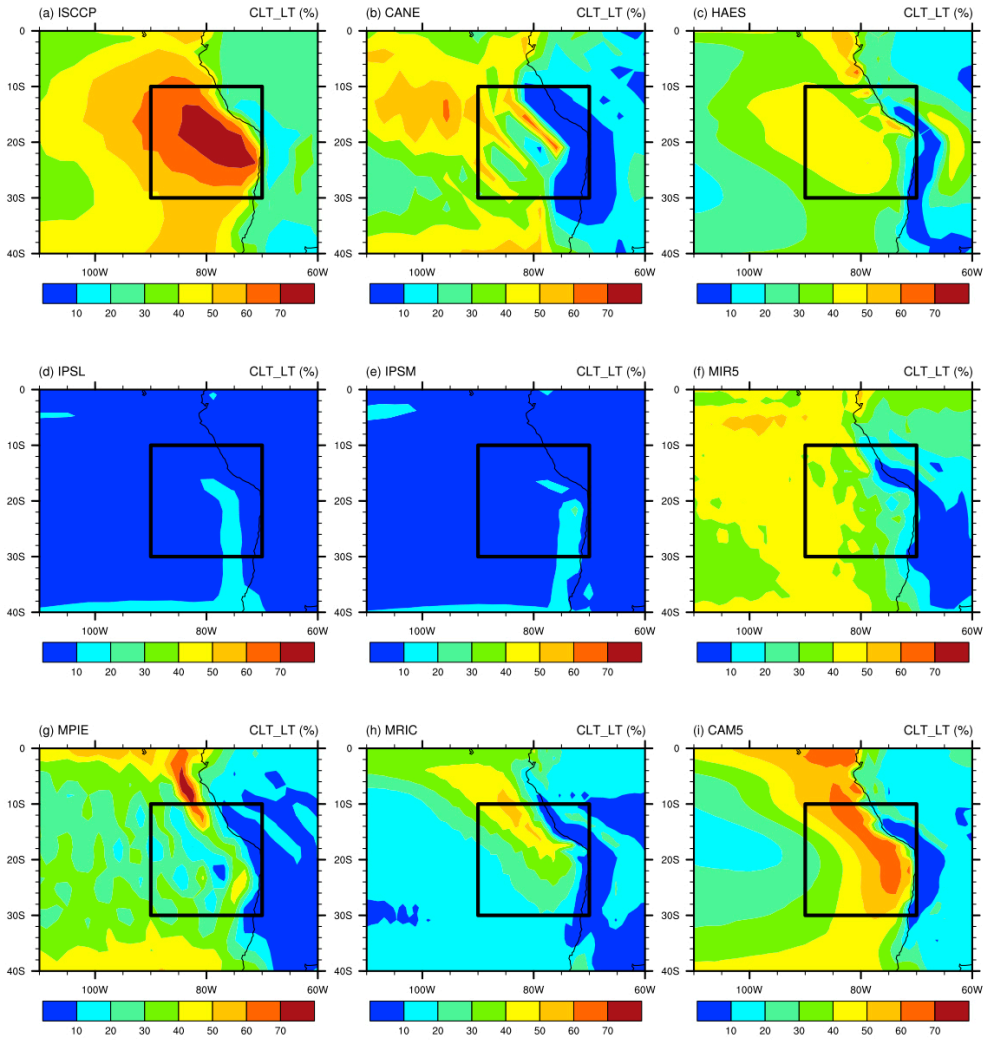

Figure 2. Horizontal map of annual mean SST for (a) observation of ISCCP, and (b)-(i) eight CMIP5/CFMIP models. The box denotes the core stratocumulus region (10S-30S, 70W-90W).

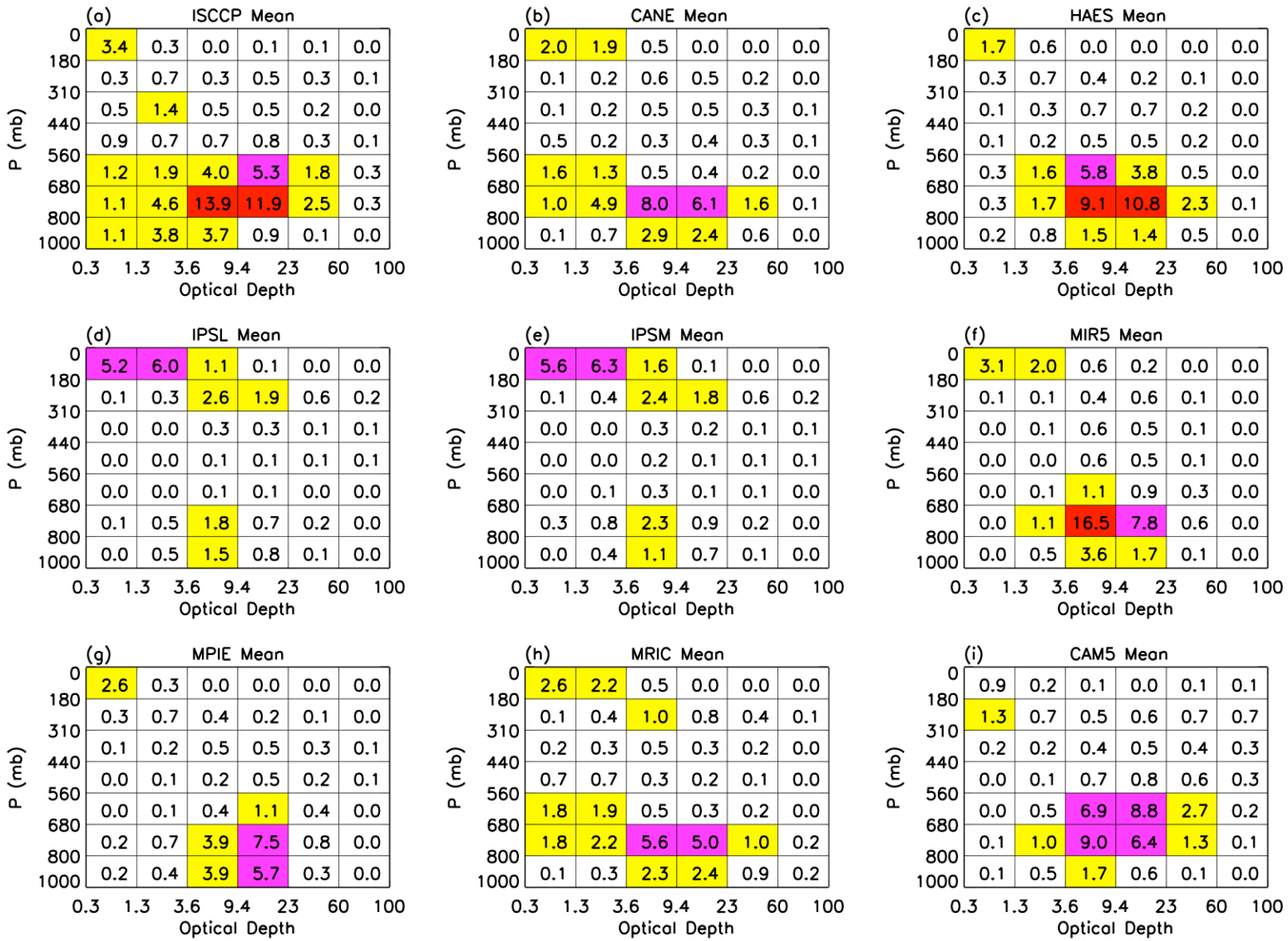

Figure 3. Ptop-τ histogram of annual mean cloud cover averaged between 10S-30S, 70W-90W. Values between 1 and 3, between 3 and 9, and larger than 9 are shaded in yellow, magneta, and red, respectively.

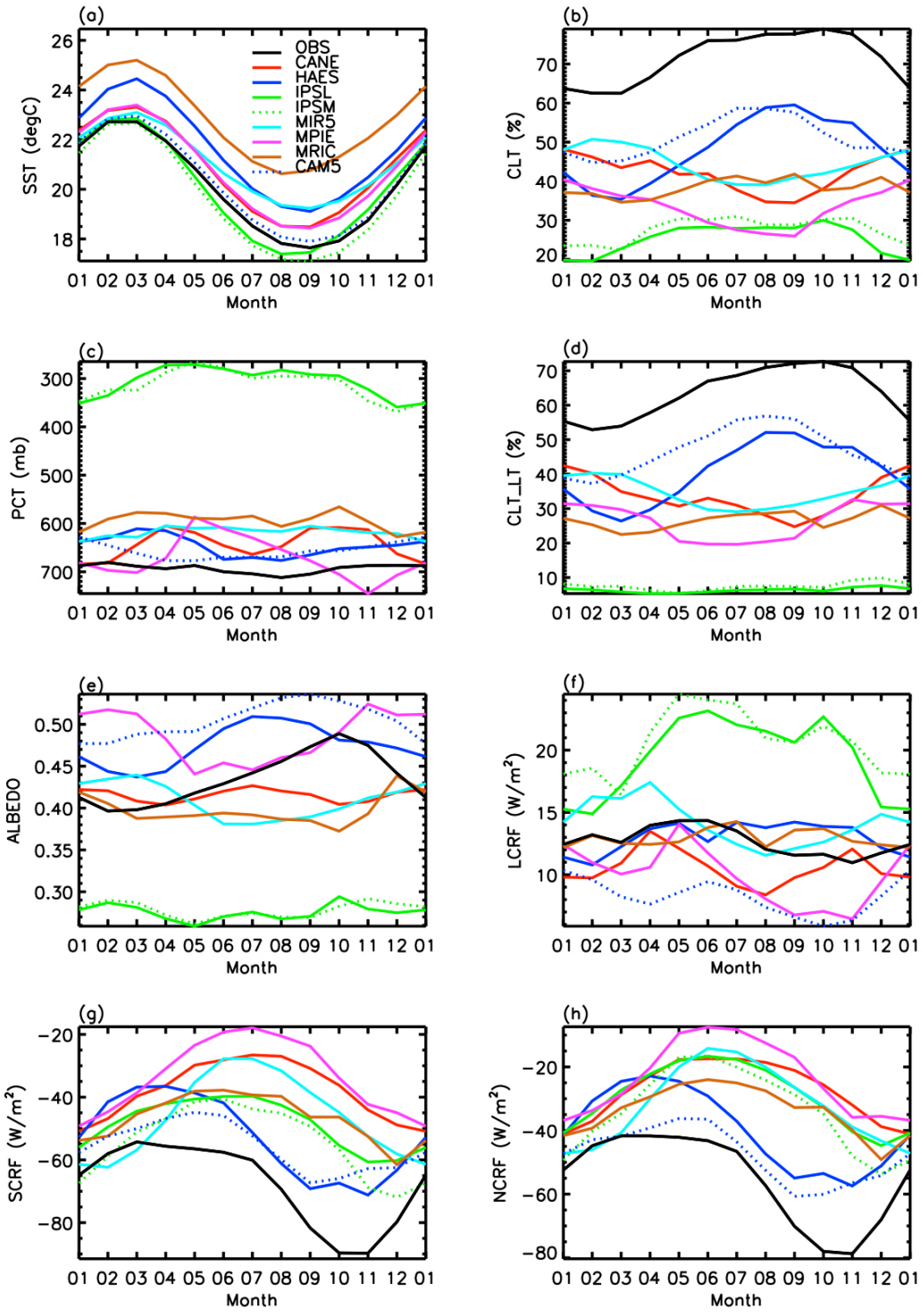

Figure 4. Seasonal cycle of (a) SST, (b) total cloud cover, (c) cloud top pressure, (d) lower troposphere cloud cover, (e) cloud albedo, (f) LWCRF, (g) SWCRF, and (h) NETCRF for observation and eight CMIP5/CFMIP models. All data are averaged between 10S-30S, 70W-90W.

(2) Cloud-radiation feedback

Figure 5 displays the vertical structure of cloud cover change associated with local SST warming. All data are averaged between 10ºS-30ºS, 70ºW-90ºW. Linear regression is calculated between the cloud fraction in each Ptop-τ pixel and local SST. In observation, there is a significant decrease of stratocumulus clouds and stratus clouds, but a slight increase of cirrus clouds associated with SST warming. Only the HAES, CAM5 and MRIC models capture the decrease of low clouds but the magnitude is too small in the MRIC model. The two IPSL models simulate a decrease of cirrus and cirrostratus clouds associated with SST warming. The CANE, MIR5 and MPIE models generally show an increase of low clouds associated with SST warming.

The linear regression coefficient shown in Figure 5 includes all the time-scales the data could cover, ranging from sub-seasonal to decadal time-scales. Next we check about the physical relationship at each different time-scales by calculating the cross-spectrum and regression between cloud/radiation variables and the local SST. Figure 6 shows the cross-spectrum and lag-0 regression between LTCC and SST for observation and the models. For coherence squared, the dashed line denotes the 95% confidence level. Phase difference is plotted in dots for only the frequencies with coherence squared higher than the 95% confidence level. A positive (negative) phase difference means LTCC lags (leads) SST at that time-scale. The observed cloud feedback at sub-annual to decadal time-scales is characterized by reduction of cloud cover, cloud albedo and shortwave CRF associated with local SST warming, leading to a positive cloud feedback. Only two of the eight models (HAES and CAM5) capture the observed cloud feedback.

(3) Connection with large-scale environment and model physics

The cloud and radiation biases in the models are associated with model biases in both large-scale environment and model physics. For large-scale environment, the models simulate reasonable large-scale subsidence (Figure 7) and humidity structure (Figure 8), but show problems in simulating the temperature structure (Figure 9) including missing temperature inversion, insufficient LTS, and insufficient reduction of LTS with local SST warming. For model physics, six of the eight models can simulate the increase of low cloud cover associated with larger LTS, but the regression coefficient is generally too small with only one model capturing the observed magnitude (Figure 10).

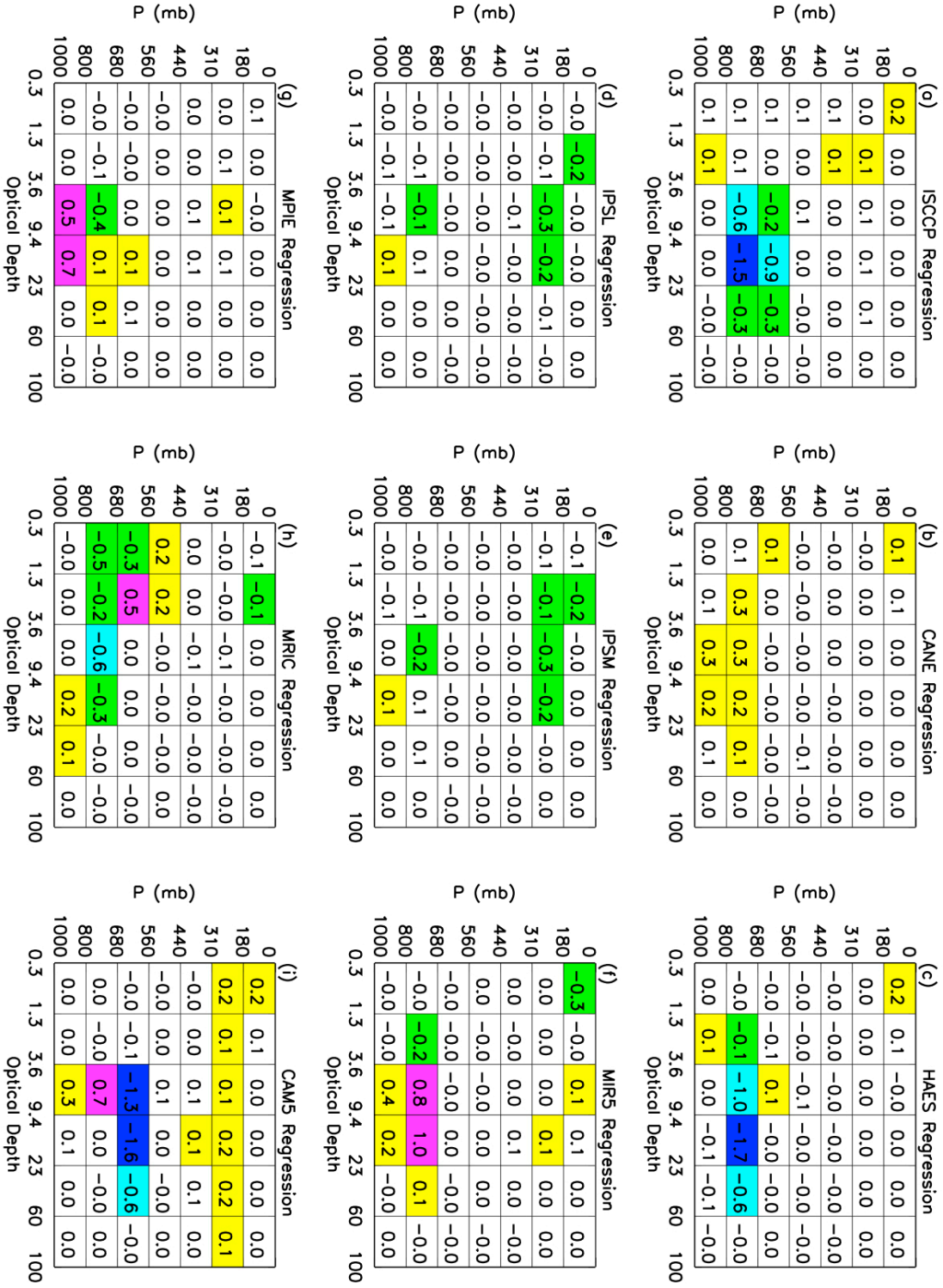

Figure 5. Linear regression of the Ptop-τ histogram to SST. All data are averaged between 10S-30S, 70W-90W. Positive values between 0.1 and 0.3, between 0.3 and 0.9, and larger than 0.9 are shaded in yellow, magneta, and red, respectively. Negative values between -0.1 and -0.3, between -0.3 and -0.9, and smaller than -0.9 are shaded in green, cyan, and blue, respectively.

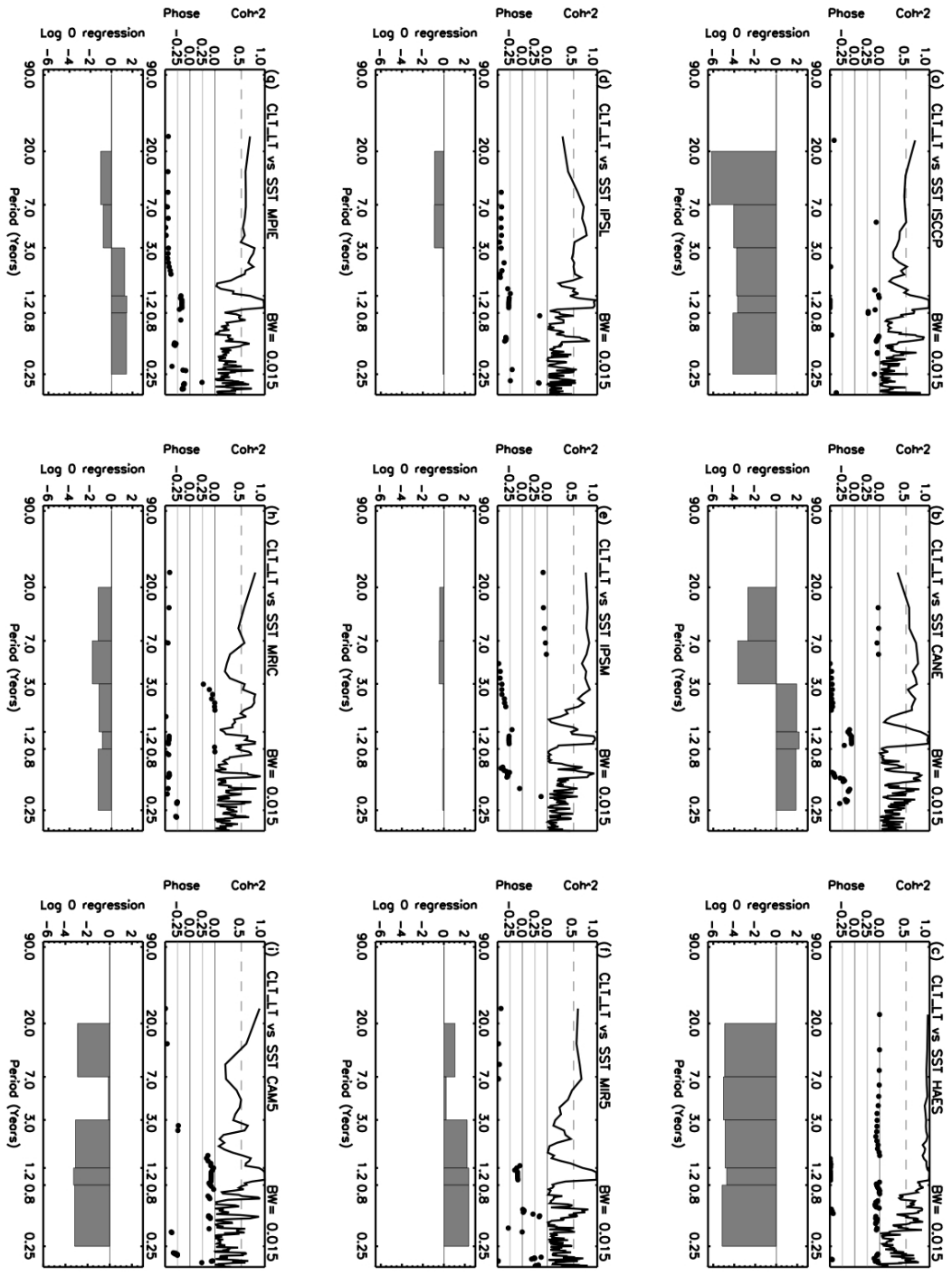

Figure 6. Coherence squared (Coh^2), phase difference, and lag-0 regression coefficients at different time-scales between low cloud cover and SST for (a) observation, and (b)-(i) eight CMIP5/CFMIP models. All data are averaged between 10S-30S, 70W-90W. For coherence squared, the dashed line denotes the 95% confidence level. Phase difference is plotted in dots for only the frequencies with coherence squared higher than the 95% confidence level. A positive (negative) phase difference means low cloud cover lags (leads) SST at that time-scale.

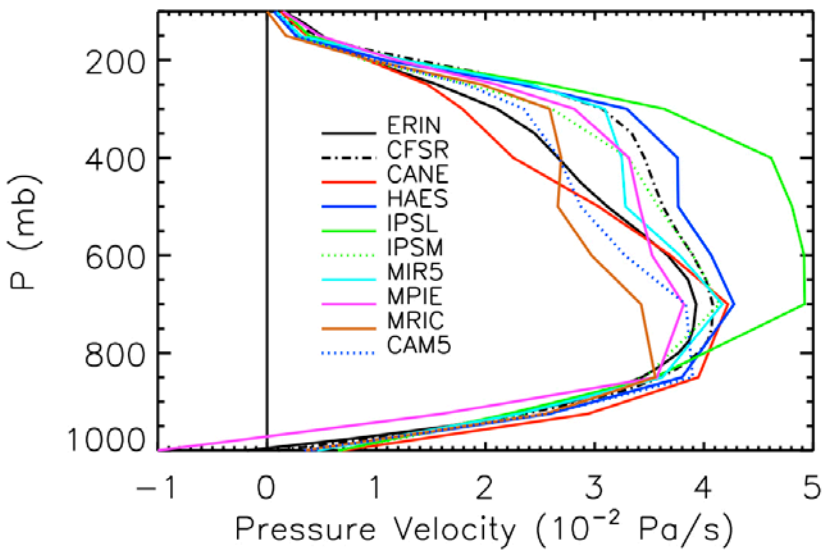

Figure 7. Vertical profile of annual mean vertical velocity for two reanalysis datasets (ERA-Interim and CFSR) and eight CMIP5/CFMIP models. All data are averaged between 10S-30S, 70W-90W.

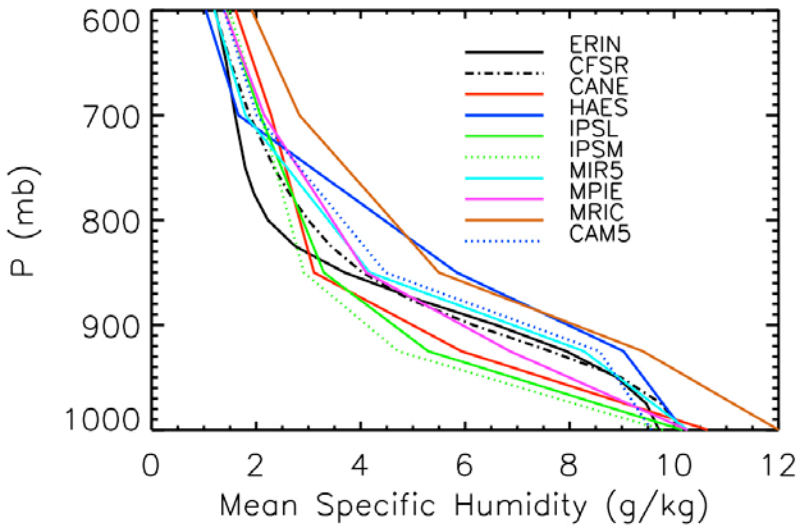

Figure 8. Same as Figure 7 but for specific humidity.

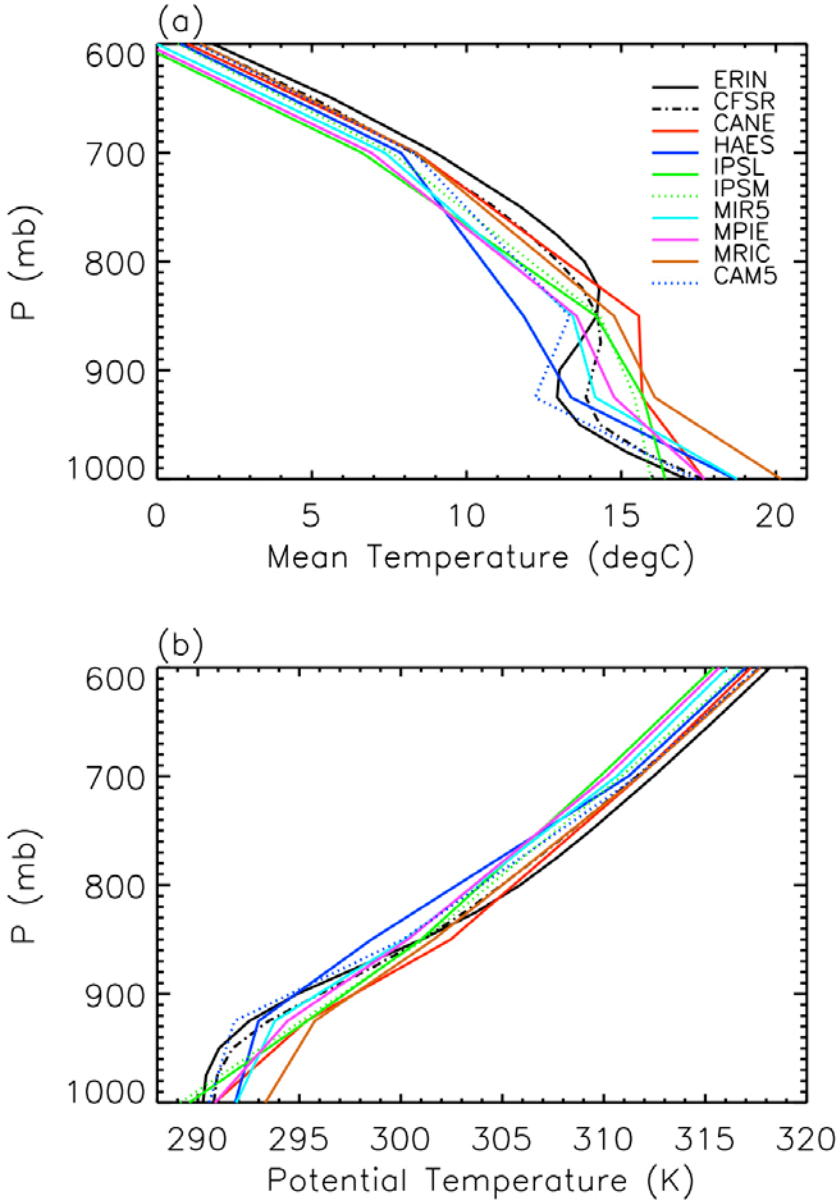

Figure 9. Same as Figure 7 but for annual mean (a) temperature, and (b) potential temperature.

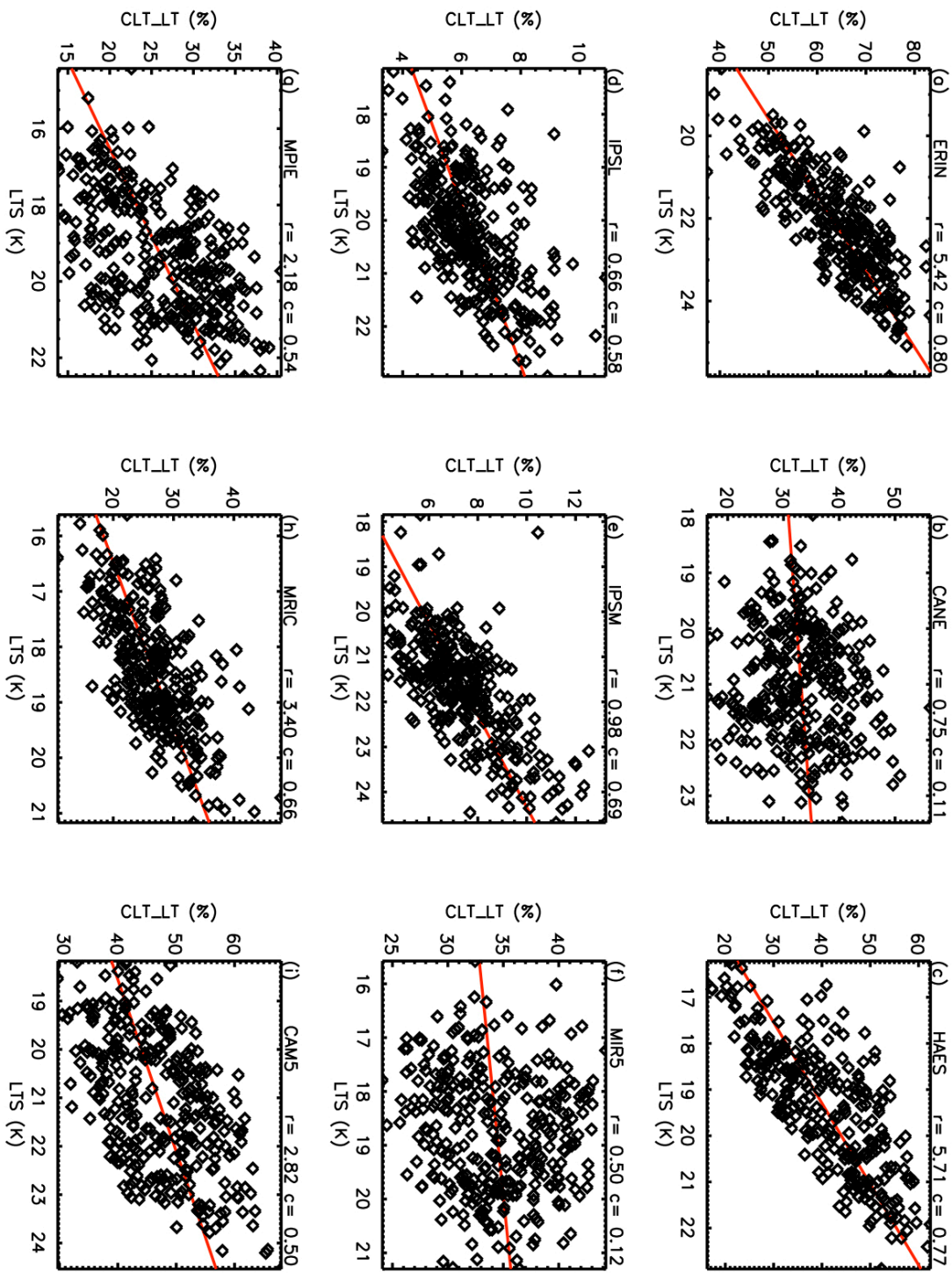

Figure 10. Scatter plot between LTS and LTCC for observation (ERA-Interim LTS vs ISCCP LTCC) and eight models. All data are averaged between 10S-30S, 70W-90W. The linear regression coefficient (r, in K/%) and correlation coefficient (c) are also shown on the top of each panel.

4. Peer-reviewed Publications

Frierson, D., D.-H. Kim, I.-S. Kang, M.-I. Lee, and J. L. Lin, 2011: Structure of AGCM-Simulated Convectively Coupled Kelvin Waves and Sensitivity to Convective Parameterization. *J. Atmos. Sci*., 68, 26-45.

Hung, M.-H., J. L. Lin, W. Wang, D. Kim, T. Shinoda, and S. Weaver, 2013: MJO and Convectively Coupled Equatorial Waves Simulated by CMIP5 Climate Models. *J. Climate*, 26, 6185-6214.

Lin, J. L., Toshiaki Shinoda, Taotao Qian, Weiqing Han, Paul Roundy, and Yangxing Zheng, 2010: Intraseasonal variation of precipitation over the western United States simulated by 14 IPCC AR4 coupled GCMs. *J. Climate*, 23, 3094-3119.

Lin, J. L., T. Qian, and T. Shinoda, 2013: Stratocumulus Clouds in Southeastern Pacific Simulated by Eight CMIP5/CFMIP Global Climate Models. *J. Climate*, accepted with major revisions.

Lin, J. L., T. Qian, T. Shinoda, S. D. Schubert, and M. J. Suarez, 2013: Is the tropical atmosphere in convective quasi-equilibrium? *Nature Geoscience*, to be submitted.

Zheng, Y., J. L. Lin, and T. Shinoda, 2012: The equatorial Pacific cold tongue simulated by IPCC AR4 coupled GCMs: Upper ocean heat budget and feedback analysis. *J. Geophy. Res*., 117, C05024, doi:10.1029/2011JC007746.

Zheng, Y., T. Shinoda, J. L. Lin, and G. N. Kiladis, 2011: Sea Surface Temperature Biases under the Stratus Cloud Deck in the Southeast Pacific Ocean in 19 IPCC AR4 Coupled General Circulation Models. *J. Climate*, 24, 4139-4164.